Bull. Chem. Soc. Jpn., ***69***, 1509—1516 (1996)

Fischer–Tropsch Synthesis with Supported Cobalt Catalyst. Promoting Effects of Lanthanum Oxide for Cobalt/Silica Catalyst

Michiaki Adachi, Kiyotaka Yoshii, Yi Zhuo Han, and Kaoru Fujimoto*

Department of Applied Chemistry, Graduate School of Engineering, The University of Tokyo,
7-3-1, Hongo, Bunkyo-ku, Tokyo 113

(Received November 29, 1995)

The promotional effects of metal oxides for a silica-supported cobalt catalyst were investigated by using X-ray diffraction (XRD), Transmission Electron Microscopy (TEM), Temperature Programmed Reaction (TPR), and Fourier Transform-Infrared Spectroscopy (FT-IR) techniques. The La-modified cobalt catalyst with 3% La loading which was prepared by simultaneous impregnation showed higher catalytic activity while keeping slightly higher selectivity of C_{2+} hydrocarbons. TPR, FT-IR, and TEM studies revealed that CO is adsorbed on the La-modified cobalt catalyst in a more active state compared to the monometallic cobalt catalyst, which was caused by the agglomeration of cobalt.

Cobalt catalysts were used since the 1930's for the commercial Fischer–Tropsch (F–T) synthesis for making liquid fuels from coal. The characteristic features of cobalt catalysts are that[1—4] (1) they make little carbon dioxide, (2) they are quite active at low temperature, (3) they make paraffinic hydrocarbons but few oxygenates, (4) they give higher methane selectivity at high temperature.

Recently, a variety of trials[5—9] have been conducted to modify the undesirable characteristics of cobalt catalysts while keeping their merits. In 1993, Shell Group succeeded in commercialization of the cobalt catalyzed F–T synthesis for making liquid fuels from natural gas.[10] Iglesia et al.[11] pointed out that hydrocarbon synthesis rates on Co catalyst were proportional to metal dispersion and independent on the metal oxide support (SiO_2, Al_2O_3. TiO_2, and ZrO_2-modified SiO_2 and TiO_2), while the C_{5+} selectivity (hydrocarbons with five or more carbon atoms) was slightly dependent on the dispersion or the support. Their further study on the promoted catalyst clarified that the addition of small amounts of Ru to Co/TiO_2 or Co/SiO_2 catalysts promoted their turnover rate by a factor of three and also C_{5+} selectivity in the F–T synthesis.[12] Also, deactivated bimetallic Co–Ru catalysts could be regenerated by a hydrogen treatment at reaction temperature whereas monometallic Co catalyst could not. Bruce et al. studied the promoting effect of ruthenium over coprecipitated cobalt/ceria catalyst to show that the ruthenium promotion increased the activity by threefold without changing the selectivity and suppressed the deactivation. They concluded that the added ruthenium-promoted the reduction of cobalt to result in more cobalt metal during the reaction.[13] Viswanathan et al.[14] studied the effect of kieselguhr and thoria to clarify that the encapsulation of cobalt oxide particles by kieselguhr occurs during hydrogen reduction, which supposed either coagulation or reduction, while thoria promoted the reduction of cobalt due to the hindered migration of kieselguhr.

The promoting effect of zirconia on cobalt catalyst has been attracting attention recently. Oukaci et al.[15] reported that a zirconia addition resulted in at least a twofold increase in activity. Shell's patents[15,16] indicated that the zirconia addition to supported cobalt catalyst increased the overall activity for F–T synthesis without affecting the selectivity of higher hydrocarbons. The promoting effects of zirconia were also found in Co/SiO_2 or Co/Al_2O_3 and a cobalt carbonyl-derived catalyst for F–T synthesis by Withers et al.[18] However, the effect of Zr on either physical structure or electronic structure has never been clarified.

In the present work, we found that La-promoted cobalt catalyst supported on silica gel shows excellent catalytic activity for F–T synthesis and has almost no effect on the selectivity for higher hydrocarbons. The La-promoted cobalt catalyst is characterized by using spectroscopic and physical-chemical methods.

Experimental

Catalyst Preparation and Characterizations. a. Catalyst Preparation and Activation. The supported cobalt catalysts used in this study were prepared by impregnating cobalt(II) nitrate on a commercially available silica gel (ID gel, Fuji Davison, specific surface area: 127 $m^2 g^{-1}$ and pore volume: 0.69 $cm^3 g^{-1}$), drying in air at 393 K for 12 h, then calcinating at 623 K for 3 h. The lanthanum promoted catalysts were prepared by impregnating the silica gel with the mixture of cobalt(II) nitrate and lanthanum(III) nitrate, drying and calcinating under same conditions as above. Some catalysts were prepared by impregnating lanthanum(III) nitrate first, converting them into oxides and then impregnating cobalt(II) nitrate in order to find the differences with those prepared by standard methods. After calcination, catalysts were activated in flowing hydrogen at 673 K for 12 h and, then passivated by nitrogen containing 1% oxygen.

b. Adsorption Measurement and TPR of Adsorbed CO. The adsorption measurement and TPR of adsorbed CO with hydrogen were conducted in a flow-through/batch cell connected to a conventional glass vacuum system. The catalyst samples were activated following the procedure identical to that for syngas conversion and then the cell was used as batch-wise system to be evacuated at 673 K for 1h. After the evacuation samples were cooled to room temperature, exposed to 200 Torr of pure CO (1 Torr = 133.322 Pa) and then further cooled to ice-temperature under CO atmosphere and maintained at the temperature for 1/2 h to determine the amount of chemisorbed CO. The samples were then evacuated again down to 2×10^{-5} Torr at 273 K (required about 1/2 h). The TPR measurement of adsorbed CO was performed by heating the samples with pre-adsorbed CO at a heating rate of 400 K h^{-1} in flowing hydrogen and by analyzing the desorbed products with a FID gas chromatograph equipped with a methanator. The details of the method have been described previously.[20,21]

c. XRD and FT–IR Measurement. XRD spectra of the catalysts in different status, after calcination, after reduction and after reaction were obtained by using a Rigaku, RINT2400 at the measurement conditions of 2θ: 20.00°—80.00°, step: 0.010°.

IR measurements of adsorbed CO on the catalyst were conducted by using a flow through cell equipped with CaF$_2$ windows, which was connected to a glass vacuum system. The procedure of the measurement has been given elsewhere.[22]

Reaction Apparatus and Procedures. All reactions were carried out in a conventional fixed-bed reactor (made of stainless steel, i.d. 6 mm, o.d. 8 mm, H. 50 mm) connected with a high-pressure gas-flow controller system. The passivated catalyst (2 g, 20—40 mesh) was diluted by the same volume of quartz sand and this mixture was packed in the reactor. After we purged the system with nitrogen, hydrogen was introduced into it and the tem-

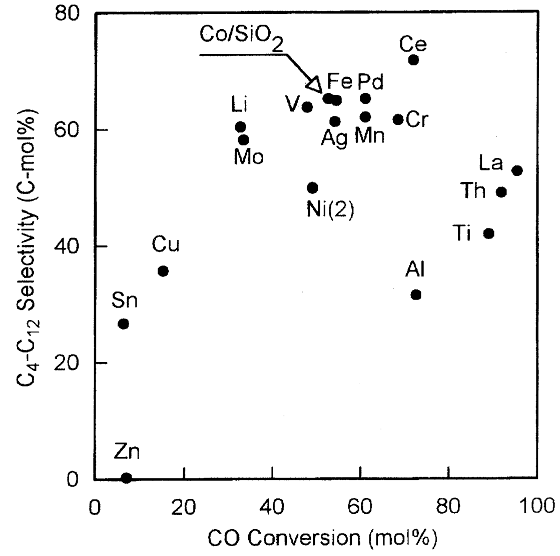

Fig. 1. Effect of metal addition on Co/SiO$_2$ catalyst. 503 K, 0.6 MPa, 10 g-cat.-h/mol, H$_2$/CO = 2/1, Co loading: 10 wt%.

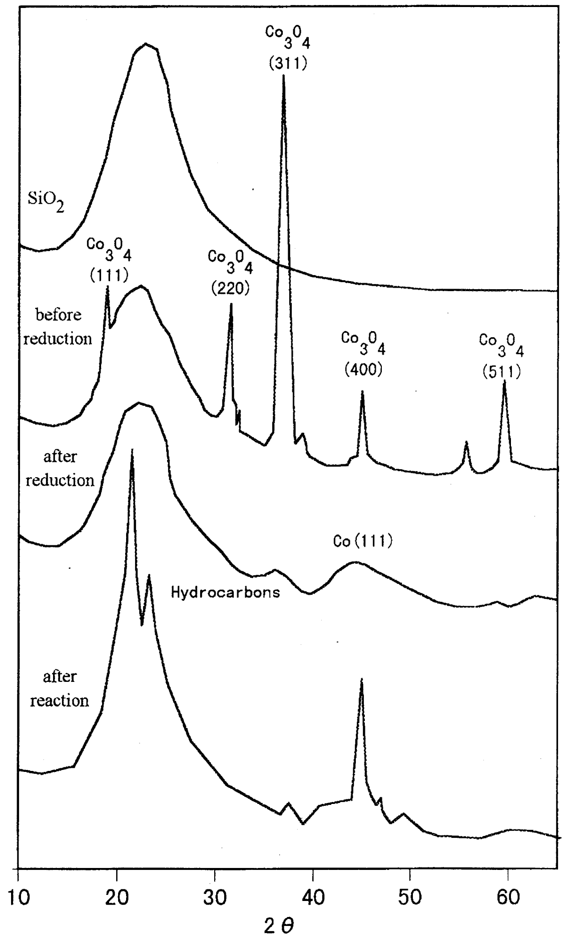

Fig. 2. XRD pattern of Co/SiO$_2$ catalyst.

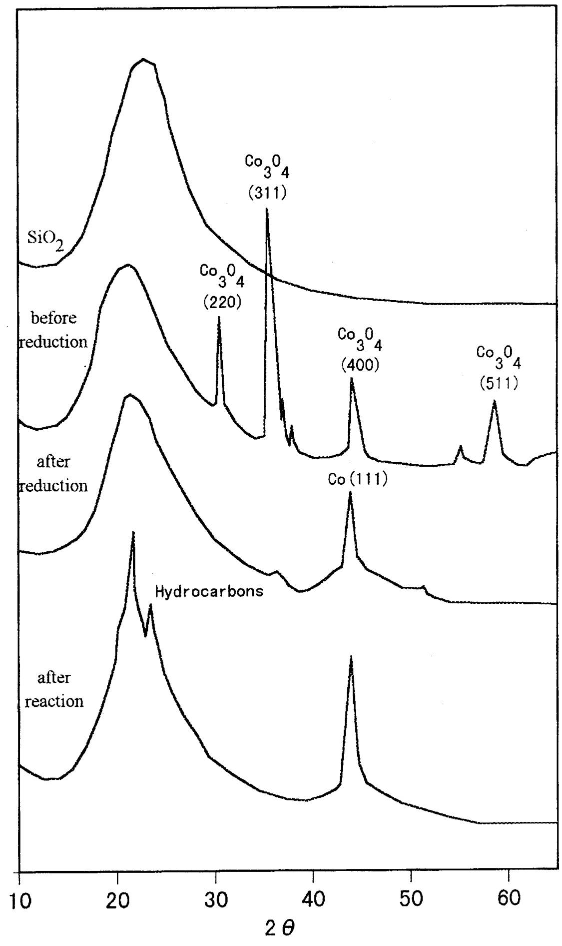

Fig. 3. XRD pattern of Co–La(3)SiO$_2$ catalyst.

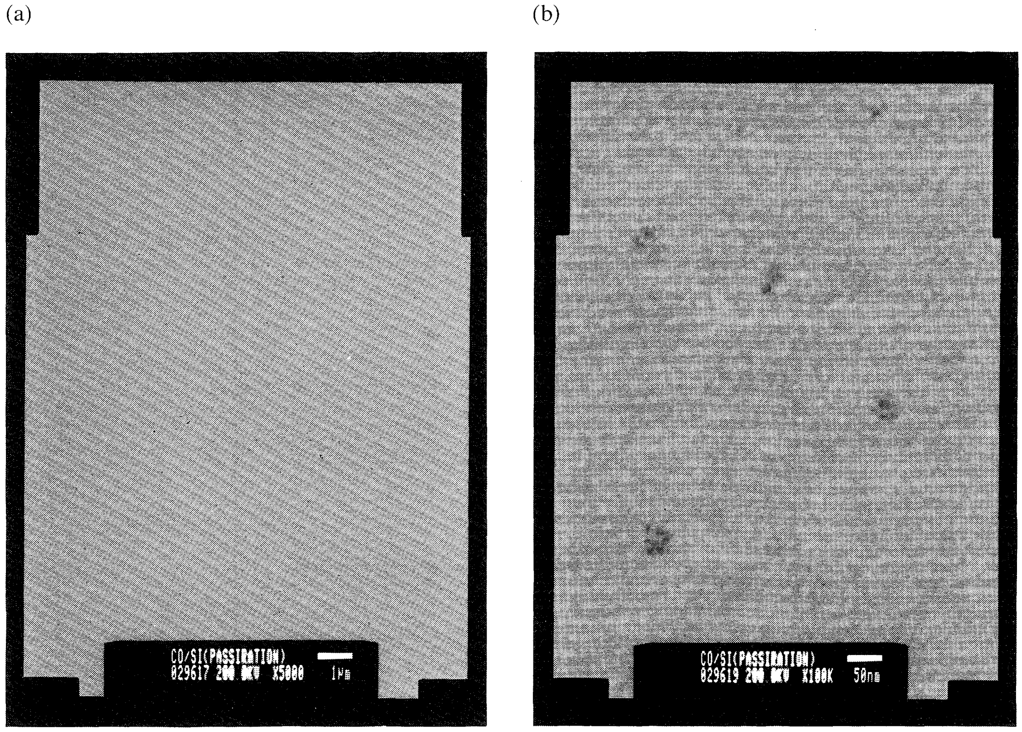

Fig. 4. TEM photographs of Co/SiO_2 catalyst (after passivation).

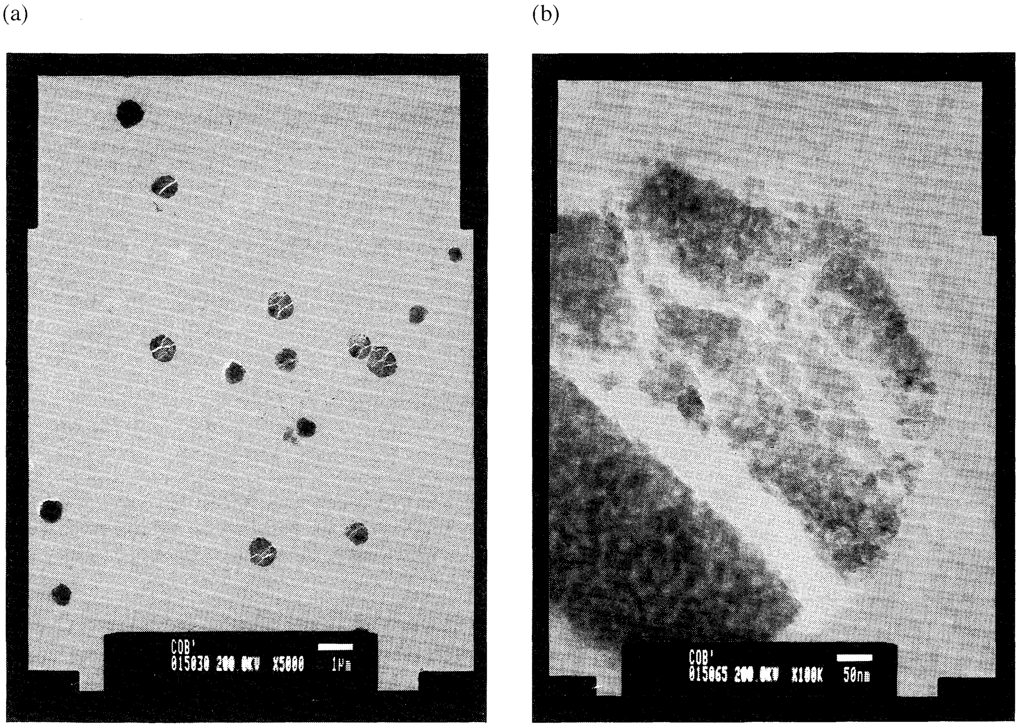

Fig. 5. TEM photographs of Co–La(3)/SiO_2 catalyst (after passivation).

perature was raised from room temperature to 673 K at a rate of 5 K min^{-1}, then kept at the temperature for 2 h to reduce the passivated catalyst. After the reduction, the temperature was lowered to reaction temperature, and then syngas was introduced instead of nitrogen. During the reaction, the effluent gas released from the back pressure regulator was introduced to a heated sampling valve for gas chromatograph analysis to determine the carbon number distribution. The effluent gas was also cooled further at an ice trap to remove the water and condensable products, then uncondensed gas was analyzed by gas chromatograph to determine CO, CO_2, and CH_4. After the reaction operation, the product which remained in the catalyst bed was extracted by supercritical hexane at 513 K for 3 h. The extracted products were also analyzed by another gas chromatograph.

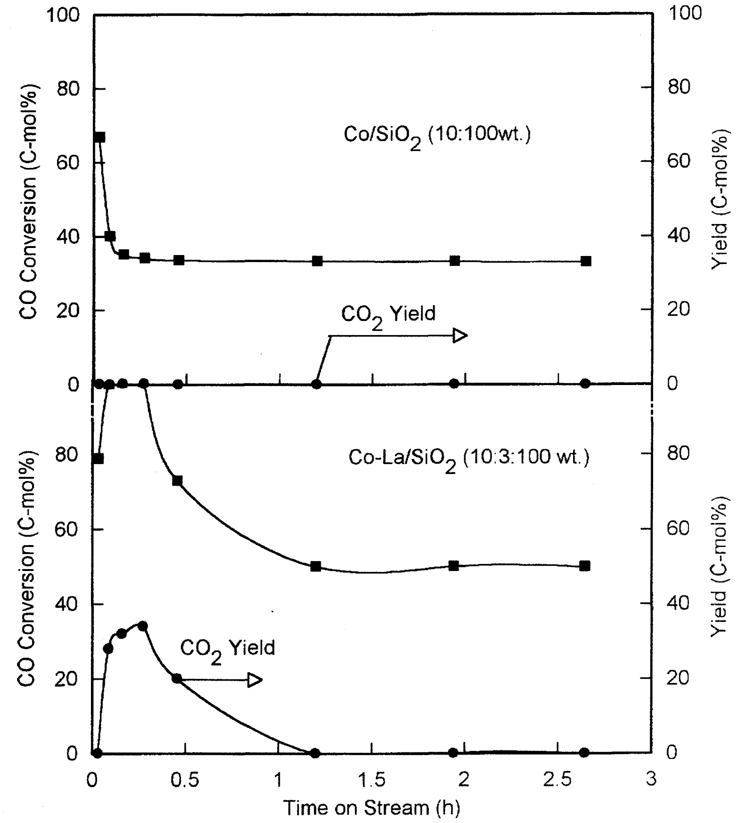

Fig. 6. Activity change of Co–La(3)/SiO$_2$ catalyst with time on stream. 513 K, 1.1 MPa, 6.7 g-cat.h/mol, H$_2$/CO = 2/1.

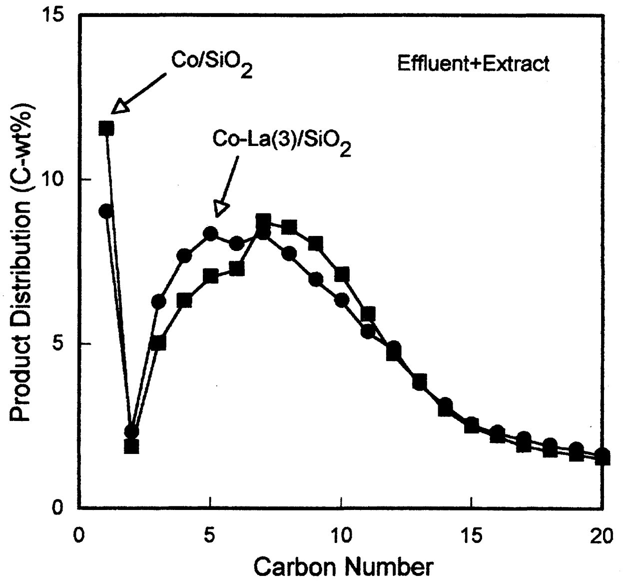

Fig. 7. Product distribution on Co/SiO$_2$ and Co–La(3)/SiO$_2$ catalyst. 503 K, 0.6 MPa, 10 g-cat.h/mol, H$_2$/CO = 2/1.

Table 1. Activity and Selectivity on Co–La/SiO$_2$ Catalyst

Catalyst	Co/SiO$_2$	Co–La(3)SiO$_2$	Co–La(10)SiO$_2$
CO Conversion (%)	33.0	44.3	36.0
Distribution (C-mol%)[a]			
C$_1$	16.1	12.0	12.7
C$_{2-4}$	18.5	25.7	24.6
C$_{5-11}$	58.7	58.6	59.4
C$_{12+}$	6.50	3.20	3.10
Olefin/Paraffin			
C$_3$	3.60	3.90	3.90
C$_4$	2.30	2.60	2.60

Reaction conditions: 503 K, 0.6 MPa, W/F: 10 g-cat.-h/mol, H$_2$/CO = 2/1 a) based on the effluent product during the reaction (excluding the product trapped in the catalyst bed).

Results and Discussion

a. Catalytic Features of Modified and Unmodified Co/SiO$_2$ Catalysts. Figure 1 shows the activity and selectivity (selectivity of C$_4$—C$_{12}$ hydrocarbons, 2 h after start of the reaction) of a variety of Co–Metal/SiO$_2$ catalysts. The hydrocarbons shown in this figure are the major part of C$_{4+}$ hydrocarbons in the effluent from the back pressure regulator which was kept at 423 K. Although the values are different from the real distribution of product hydrocarbons shown in the later figures, the catalyst which gave the higher ratio of C$_4$–C$_{12}$ fraction in effluent to the total hydrocarbons can be considered as the catalyst giving high chain growth ability. It is clear that the effects of additives can be divided into several groups: the first one consists of those which suppress both activity and selectivity. The next includes those which improve mainly selectivity (Ce). The third one includes those improve the activity while having almost no effect on the selectivity (La, Th, Ti). Among these additives, Th has been known as an excellent additive since the 1930's.[1,4)] In

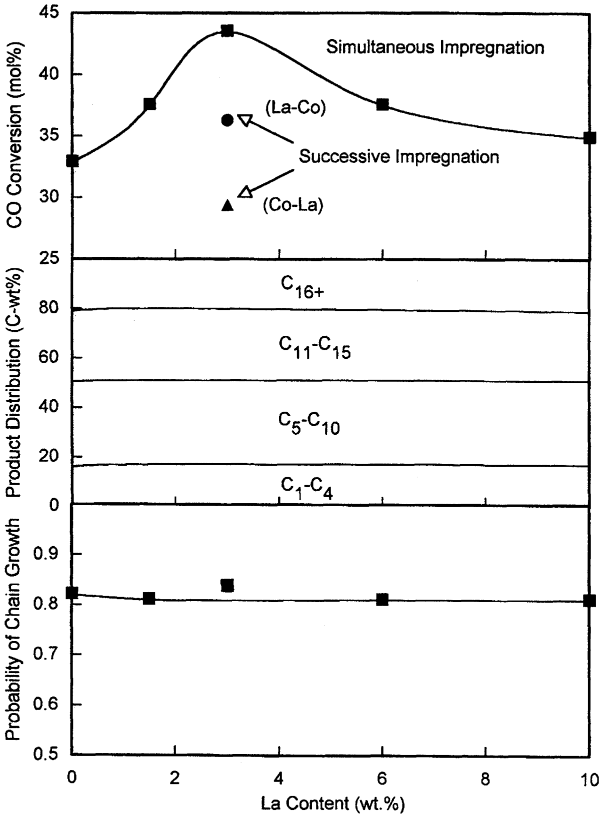

Fig. 8. Effect of La loading on Co–La/SiO$_2$ catalyst. 503 K, 0.6 MPa, 10 g-cat.-h/mol, H$_2$/CO = 2/1.

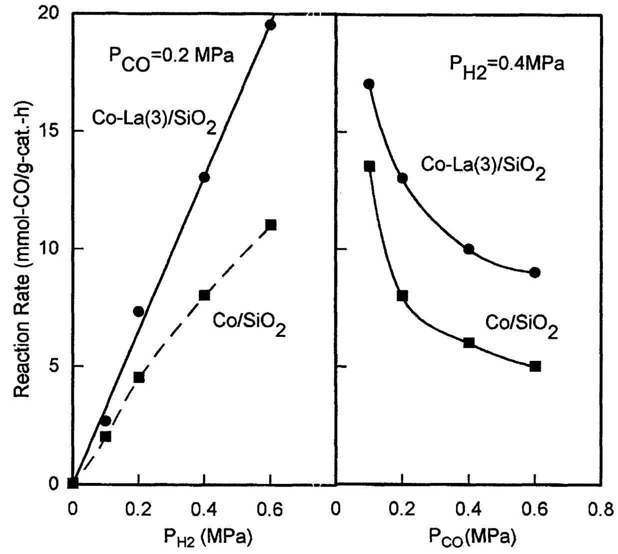

Fig. 9. Reaction rate as a function of H$_2$ and CO partial pressure. 503 K, 2.0 g-cat.-h/mol, Co–La(3)/SiO$_2$.

the present study, La was selected as the additive in order to clarify the mechanism for promoting the catalytic activity while leaving the selectivity unchanged.

b. Catalyst Structure before and after the Reaction. Figures 2 and 3 show the XRD patterns of Co/SiO$_2$ and Co–La(3)/SiO$_2$ catalysts after calcination, after hydrogen reduction and after reaction. From these figures, one can see that fine crystals of Co$_3$O$_4$ were formed in each catalyst during the calcination in air, in agreement with other researchers' reports.[23—25] The reflect peaks of Co$_3$O$_4$ disappear after reduction in hydrogen at 673 K for 12 h, indicating that oxides were completely reduced. The peaks of Co(111) differs from each other greatly. For Co/SiO$_2$ catalyst, the peak is quite broad, which suggests that the crystal size of Co is quite small (ca. 5 nm), whereas the Co crystals on La-promoted catalyst are a mixture of large crystals and small crystals. After the reaction, the broad peak of Co(111) becomes a sharp peak at 46° for both catalysts which suggests that the crystals grew during the reaction, especially for unpromoted catalyst. On the other hand, no apparent peaks attributed to La$_2$O$_3$ can be found. However, La(NO$_3$)$_3$ has been known to be converted to La$_2$O$_3$ by air calcination at 723 K, and it is hard to be reduced to lower valence lanthanum oxide by hydrogen treatment at 673 K.[26] Therefore, it is most probable that the crystals of La$_2$O$_3$ are quite finely (<3 nm) dispersed on silica surfaces.

TEM photographs of promoted cobalt and unpromoted catalysts are shown in Figs. 4 and 5. It is clear from the photographs that fine Co particles (ca. 10 nm) are uniformly distributed in the Co/SiO$_2$ catalyst, whereas the large Co particles exist in the Co–La(3)/SiO$_2$ catalyst. However, the large particle is not a single crystal but a cluster composed of small crystals, which indicates that some agglomeration occured during the calcination in air, along with the TEM measurement of calcinated catalysts, but the small crystals did not fuse into a single crystal. On the other hand, particles of La$_2$O$_3$ were not identified by either XRD or high magnification TEM, proving that La$_2$O$_3$ is dispersed quite finely on silica gel. When the surface of silica gel is modified with lanthanum ion, the interaction between Co ion and SiO$_2$ surface will be weakened. This will result in promoting the migration of Co$_3$O$_4$ particles during the calcination in air.

c. Catalytic Properties and Effects of La Addition. Catalytic activities of Co/SiO$_2$ and Co–La(3)/SiO$_2$ (prepared by simultaneous impregnation) are shown in Fig. 6 as a function of reaction time. This figure shows that the two catalysts have quite different characteristic features. The activity of unpromoted catalyst decreases very quickly within the initial 10—20 min and then the steady state is obtained, whose values decreases gradually (probably because of wax deposition). On the other hand, the La-promoted catalyst shows a similar activity to the former one at the beginning of the reaction. Then, it rises quickly to reach 100% of CO conversion, while giving a large amount of CO$_2$. This may be caused by the reaction of CO with the oxygen formed via the decomposition of adsorbed CO, the so-called Bourdard reaction. This means that the La-modified catalyst has a high activity for decomposing CO. However, the Bourdard reaction causes carbon deposition which poisons the surface of cobalt and lowers the activity. After about 1 h, it seems to reach the steady state activity level. Meanwhile, the formation of CO$_2$ stopped. The steady state activity is higher by only 30% than that of La-free catalyst, this is because of the deactivation caused by carbon deposition which occured at

Table 2. CO Chemisorption on Co–La/SiO$_2$ Catalyst and TPR

La content (wt%)	0	3	3	3	10
Preparation method	—	simul.[a]	succ.[b]	succ.[c]	simul.
CO chemisorption (μmol g^{-1})	690	590	710	450	490
Dispersion (%)[d]	41	35	42	27	29
CH$_4$/CO in TPR product[e]	12	17	8.0	5.0	26
CH$_4$ desorbed temp K[f]	423	408	422	423	403
TOF (S^{-1} × 10^3)[g]	4.7	7.1	5.1	6.5	7.1

a) Simultaneous impregnation. b) Successive impregnation (La–Co). c) Successive impregnation (Co–La). d) Based on chemisorbed CO, assuming CO/Co$_{surface}$ = 1. e) Total amount. f) CH$_4$ peak temperature. g) Reaction conditions: 503 K, 0.6 MPa, H$_2$/CO = 2/1, 10 g-cat.-h/mol.

the beginning of the reaction, and the intrinsic activity should be much higher.

The product distributions are illustrated in Fig. 7. These were calculated based on the total amount of effluent products and extracted products after 8-h reaction and recalculated as carbon percentage base. The results demonstrate that both catalysts give similar products, except that Co/SiO$_2$ gives slightly higher selectivity of methane, whereas the La-modified catalyst yields more C$_2$–C$_5$ hydrocarbons. The details of activities and product distributions are tabulated in Table 1, which shows the effect of lanthanum addition to be that CO conversion increases by about 1.3 times and that the olefin content in hydrocarbons is slightly higher while the chain growth probability (α-value) calculated from C$_{10}$–C$_{20}$ hydrocarbon is quite similar at around 0.82—0.85. Thus, we can conclude that the added lanthanum oxide promoted only the catalytic activity.

Figure 8 shows the catalytic activity, product distribution and chain growth probability as a function of La content. The catalytic activity increases with increasing La loading in the range from 0 to 3% (metal base), then it decreases at loading higher than 3%. The catalyst with 10 wt% La loading has almost no differences from the La-free catalyst. These facts are similar to the case of ZrO$_2$ addition,[15—18] but different from MgO which also showed strong promotion effect but suppresses the chain growth probability.[27] It should be noted that the addition effect is marked only when La and Co were impregnated simultaneously, whereas the successive impregnation (La⟶Co) is only slightly effective in promoting the catalytic activity; another successive impregnation (Co⟶La) shows even worse effect than no addition. Table 2, which shows catalyst properties of Co/SiO$_2$ and La-promoted Co/SiO$_2$ catalysts, reveals that the simultaneously impregnated Co–La(3)/SiO$_2$ catalyst shows even smaller CO chemisorption but by 35% higher TOF (turn over frequency, based on the total amount of chemisorbed CO), which means that the average reactivity of adsorbed CO on La-modified Co catalyst is higher than on the La-free catalyst. This is also the case for Co–La (10)/SiO$_2$ catalyst, but the number of active sites (the amount of CO chemisorption) is much smaller than Co–La(3)/SiO$_2$ catalyst, giving lower apparent activity. The successive impregnation (Co⟶La) gave much smaller active sites, suggesting that a part of Co is covered by La$_2$O$_3$ on which no CO is adsorbed. Effects of La-addition will be discussed later.

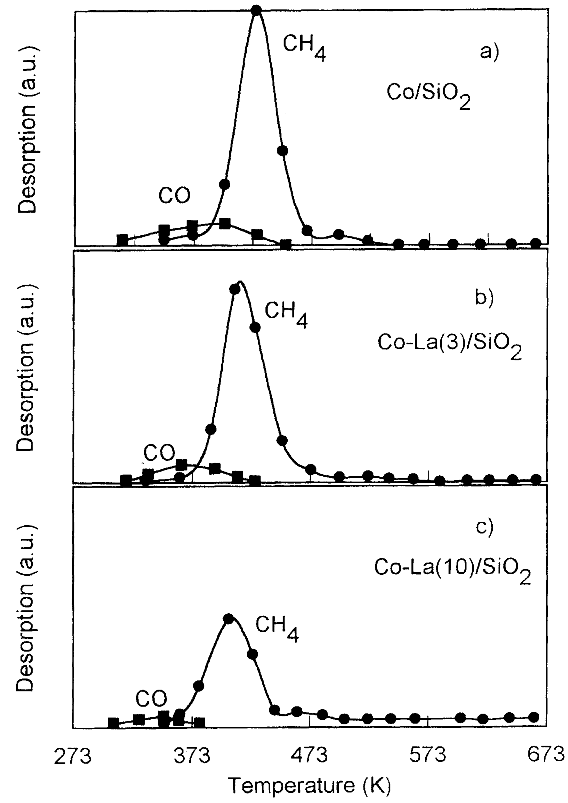

Fig. 10. TPR spectra of adsorbed CO.

The dependencies of reaction rate on partial pressures of CO and H$_2$ for either Co/SiO$_2$ or Co–La(3)/SiO$_2$ catalyst are shown in Fig. 9. Reaction orders with respect to H$_2$ partial pressure, is almost 1.0 for each catalyst. However, at high hydrogen pressure (above 0.4 MPa) the rate on the Co/SiO$_2$ catalyst is lower than the level predicted by the first-order rate equation, whereas the rate of La-modified catalyst fits the rate equation quite well. Generally,the Fischer–Tropsch reaction proceeds via the decomposition of CO to surface carbon and oxygen which is followed by the hydropolymerization of surface carbon. If the rate of CO decomposition is much higher than that of hydropolymerization, the apparent reaction order is first order with respect to hydrogen. However, when the rate of hydrogenation activity is high (for example, at high hydrogen partial pressure) and comparable to that of CO decomposition, the reaction order with respect to hydrogen is lower than 1.0. The experimental results suggest that the reaction over the La-free catalyst is in agreement with this mechanism whereas that over La-promoted catalyst is not. For the reaction order with respect to CO, the characteristic feature is that the order is strongly negative for either catalyst, while the inhibiting effect is stronger for La-free catalyst. The inhibiting effect could be attributed to the reversible coverage of active site with inactive CO. This subject will be discussed later.

d. Effect of La-Addition on the Reactivity of Adsorbed CO on Cobalt. In Fig. 10 and Table 2 are shown the TPR

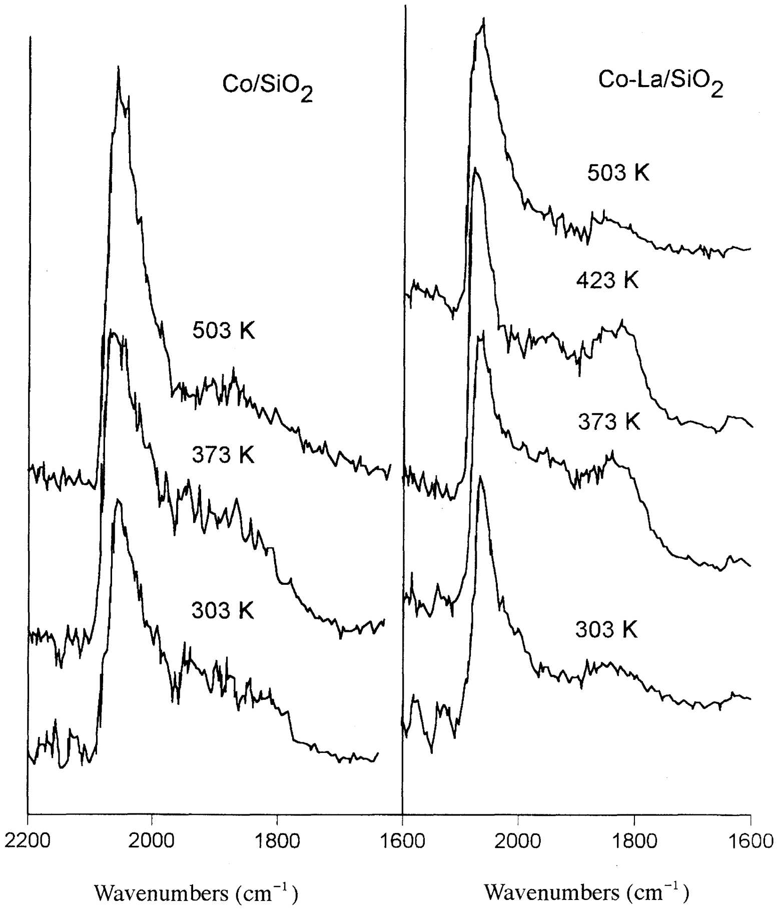

Fig. 11. FT–IR spectra of adsorbed CO.

spectra of adsorbed CO, amount of CO adsorption, Co dispersion and TOF on a variety of Co catalysts. The products of CO-TPR are CH_4 and CO. The CO peak appears at a lower temperature than that of CH_4 for each catalyst. The peak of CH_4 appears at different temperature depending on the catalyst. The characteristic features of La-modified catalyst are the decrease in peaks area of CH_4 and CO (especially CO) and the shift of CH_4 peak to lower temperature. The adsorbed CO which desorbed as CO is an inactive species for the F–T reaction which might be attributed to "linear" type adsorbed species.[22] The decrease in the CO peak area on La-modified catalyst means the decrease in the inactive CO. On the other hand, the peak temperature of CH_4 formation on CO TPR is reported to relate closely to the catalytic activity of CO hydrogenation.[22] The cobalt catalyst promoted by lanthanum gives a CH_4 peak which appears at temperature lower by 15 K than that for the La-free catalyst. This suggests that CO is adsorbed in the more reactive state on the La-promoted catalyst than on La-free catalyst and thus it shows higher catalytic activity.

In order to confirm this idea, FT–IR measurements were conducted; results are illustrated in Fig. 11. Under syngas atmosphere, CO is adsorbed in two types: the linear type (2000—2100 cm^{-1}) and the bridge form (1830—1850 cm^{-1}). It is apparent from Fig. 11, that the formation of bridge-type adsorbed CO is favored for the La-containing catalyst, whereas the linear type CO is prevalent on La-free catalyst. As has been pointed out, the bridge-type CO is much more active than linear CO.[2] The high reactivity of adsorbed CO on La-containing catalyst can be attributed to the increase in the bridge-type adsorbed CO which is easily dissociated to carbon and oxygen and leads to the increase in its TOF.

Discussion on the Role of Lanthanum Promoter. As we pointed out in the introduction section, many types of additives have been claimed to be effective as the promoter for cobalt catalyst. For example, ZrO_2 is effective for promoting the TOF of cobalt catalyst, but the reason of its promotion is not yet clear. Lanthanum oxide was also found to be effective for promoting TOF, while the product selectivity was unchanged. The promotion effect of lanthanum, which is assumed to exist as La_2O_3, generates only when it is simultaneously deposited on the support. The significant difference between the promoted and the un-promoted catalyst is the degree of crystal size of cobalt as recognized by XRD and TEM. Pre-deposited La_2O_3 has no effect in the crystal growth and the successively added La_2O_3 exhibits no effect for promoting TOF as demonstrated in Table 2. The effects of La_2O_3 promoter other than the crystal growth include 1) higher catalytic activity, 2) the lower TPR peak of adsorbed CO, 3) higher CH_4/CO ratio in TPR experiment. These phenomena suggest clearly that the adsorbed CO on the promoted catalyst is much higher in its reactivity than that on the unpromoted one. The higher reactivity of adsorbed CO should be attributed to the higher ratio of "bridge type" CO to "linear type" CO, as exhibited in the IR spectrum in Fig. 11. Naturally, the "linear" and "bridge" type CO are convertible to each other. It is hard to specify each site, but it can be said that the fraction of reactive CO is higher on the promoted catalyst. On the unpromoted catalyst, however, where the fraction of inert CO ("linear" CO) is higher, the catalytic activity is easy to be suppressed by CO because its concentration increase with the increase in its concentration in the gas phase suppresses the access of hydrogen to active site.

The reason of the promoter effect will be the aggregation of cobalt during the air calcination. The post-addition of La_2O_3 to Co/SiO_2 causes the increase in CH_4/CO ratio in TPR only slightly but probably covers a part of cobalt, as demonstrated by the decrease in the amount of CO chemisorption.

Conclusions. The present study on the modification of cobalt catalyst proved the following:

1. The suitable amount of lanthanum addition (3 wt%, metal base) can promote the catalytic activity silica-supported cobalt catalyst and can suppress the methane formation.

2. The results of TPR of adsorbed CO with hydrogen and the FT–IR study revealed that carbon monoxide adsorbed CO on La-modified cobalt catalyst is in the more active state than on monometallic cobalt catalyst because of the larger cobalt crystal.

3. La-addition weakens the interaction between Co oxide and SiO_2 to promote the migration of cobalt metal oxide during air calcination and makes clusters of fine cobalt particles.

References

1) H. H. Storch, N. Golumbic, and R. B. Aderson, "Fischer–Tropsch and Related Synthesis," Wiley, New York (1951).

2) H. Pichler, *Adv. Catal.*, **4**, 271 (1952).

3) R. B. Anderson, "Catalysis," ed by P. H. Emmett, Rheinhold, New York (1959).

4) F. Fischer and H. Tropsch, *Brennst. Chem.*, **13**, 61 (1932).

5) H. J. F. van's Blik and R. Prins, *J. Catal.*, **97**, 188 (1985).

6) K. Takeuchi, T. Matsuzaki, T. Hanaoka, H. Arakawa, and Y. Sugi, *J. Mol. Catal.*, **55**, XXXX (1989).

7) S. H. Moon and K. E. Yoon, *Appl. Catal.*, **16**, 289 (1985).

8) T. Matsuzaki, T. Hanaoka, K. Takeuchi, Y. Sugi, and M. Reinikainen, *Catal. Lett.*, **10**, XXXX (1990).

9) B. G. Johnson, C. H. Bartholomew, and D. W. Goodman, *J. Catal.*, **128**, 231 (1991).

10) P. J. A. Tijm, H. M. H. V. Wechem, and M. M. G. Senden, "The Shell Middle Distillate Synthesis Project-New Opportunities for Marketing Natural Gas," Alternate Energy'93, Colorado Springs, April 1993, pp. 27—30.

11) E. Iglesia, S. L. Soled, and R. A. Fiato, *J. Catal.*, **137**, 212 (1992).

12) E. Iglesia, S. L. Soled, R. A. Fiato, and G. H. Via, *J. Catal.*, **143**, 345 (1993).

13) L. A. Bruce, M. Hoang, A. E. Hughes, and T. W. Turney, *Appl. Catal. A, General*, **100**, 51 (1993).

14) B. Viswanathan and R. Gopalakrishnan, *J. Catal.*, **99**, 342 (1986).

15) R. Oukaci, J. G. Goodwin, Jr., G. Marcelin, and A. Singleton, *Prepr. Pap.-Am. Chem. Soc., Div. Fuel Chem.*, **39**, 1117 (1994).

16) A. Hoek, A. H. Joustra, J. K. Minderhould, and M. F. Post, UK Patent Appl. GB. 2125062 A (1983).

17) A. Hoek, J. K. Minderhould, M. F. Post, and M. F. M. Lednor, P. W. Eur. Patent Appl. EP 110449 A1 (1984).

18) H. P. Withers, Jr., K. F. Eliezer, and J. W. Mitchell, *Ind. Eng. Chem. Res.*, **29**, 1807 (1990).

19) K. Yokota and K. Fujimoto, *Fuel*, **68**, 255 (1989).

20) K. Fujimoto, M. Kameyama, and T. Kunugi, *J. Jpn. Petrol. Inst.*, **21**, 405 (1978).

21) K. Fujimoto, M. Kameyama, Y. Abe, and T. Kunugi, *J. Jpn. Petrol. Inst.*, **24**, 233 (1981).

22) L. Fujimoto, M. Kameyama, and T. Kunugi, *J. Catal.*, **61**, 7 (1980).

23) M. K. Niemela, A. O. I. Krause, T. Vaara, and J. Lahtinen, *Top. Catal.*, **2**, 45 (1995).

24) D. G. Castner, P. G. Watson, and I. Y. Chan, *J. Phys. Chem.*, **93**, 3188 (1989).

25) S.-W. Ho, M. Houalla, and D. M. Hercules, *J. Phys. Chem.*, **94**, 6396 (1990).

26) L. Fan and K. Fujimoto, *Chem. Lett.*, **1994**, 105.

27) M. K. Neimela, A. O. I. Krause, T. Vaara, and J. Lahtien, *Top. Catal.*, **2**, 45 (1995).